

Reduced-Complexity Joint Frequency, Timing and Phase Recovery for PAM Based CPM Receivers

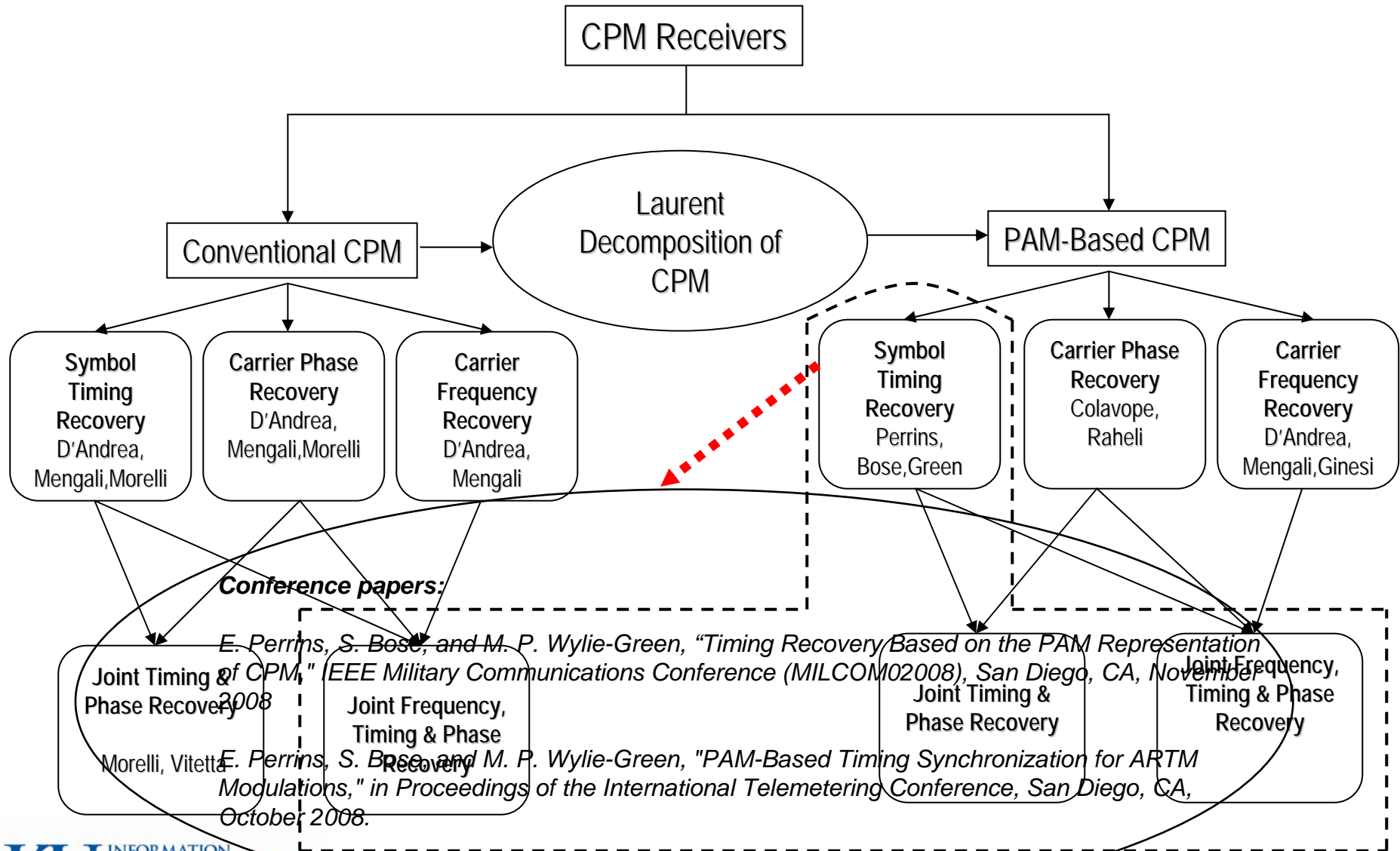
Sayak Bose

Department of Electrical Engineering and Computer Science
University of Kansas, Lawrence, Kansas

Overview

- **Introduction to Continuous Phase Modulation (CPM) related work**
- **Motivation of research**
- **Signal models and complexity reduction principle**
- **Joint timing and phase error detector (TED & PED)**
- **Effect of large frequency offsets on TED and PED**
- **Performance analysis metrics and bounds**
- **Simulation results**
- **False lock recovery using reduced complexity detector configurations**
- **Conclusions and future work**

Introduction to Continuous Phase Modulation (CPM) related work



Motivation of research

Why CPM?

- Power and bandwidth efficient.
- Easy to use with low-cost PAs.

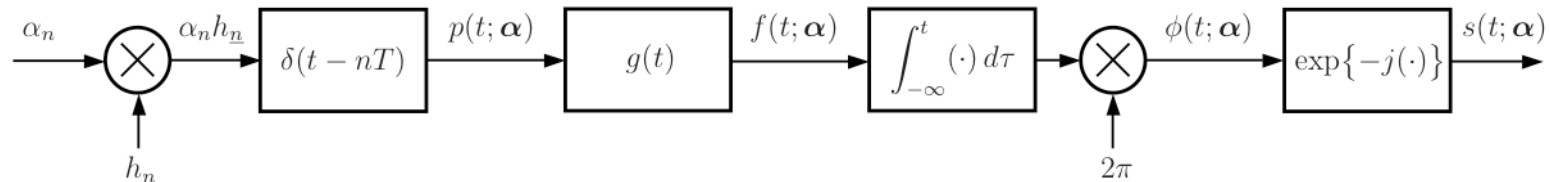
Problems with CPM

- Receiver complexity.
- Receiver synchronization.

–Motivation for using Pulse Amplitude Modulation (PAM)

- Linearize CPM; first proposed for binary CPMs in the well-known paper by Laurent.
- Reduce receiver complexity by discarding low-energy PAM pulses.
- Recover symbol timing using simple algorithms.

Conventional CPM signal model



$$s(t; \alpha) = A \exp \left\{ j2\pi h \sum_{i=0}^n \alpha_i q(t - iT) \right\}$$

- $f(t)$ is the frequency pulse, it has a finite duration of L symbol times and an area of $1/2$.
- $q(t)$ is the time-integral of $f(t)$
- h is the modulation index, it is typically a rational number
- α_n are drawn from an M -ary alphabet

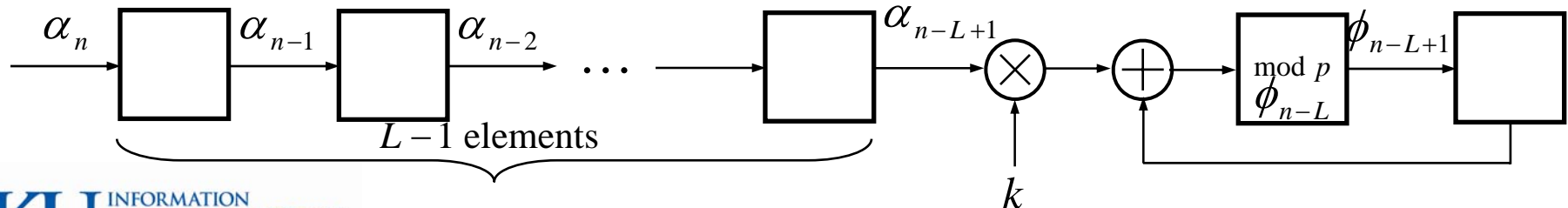
Conventional CPM signal model...contd.

- The phase can be grouped into two terms since $q(t) = 1/2$ for $t > LT$:

$$\begin{aligned} \phi(t; \alpha) &= 2\pi h \sum_{i=0}^n \alpha_i q(t - iT) \\ &= \underbrace{2\pi h \sum_{i=n-L+1}^n \alpha_i q(t - iT)}_{\phi(t; \underline{\alpha}_n)} + \underbrace{\pi h \sum_{i=0}^{n-L} \alpha_i}_{\phi_{n-L}} \end{aligned}$$

- Since the modulation indexes are rational numbers, $h=k/p$, we can describe the signal with a finite state machine:

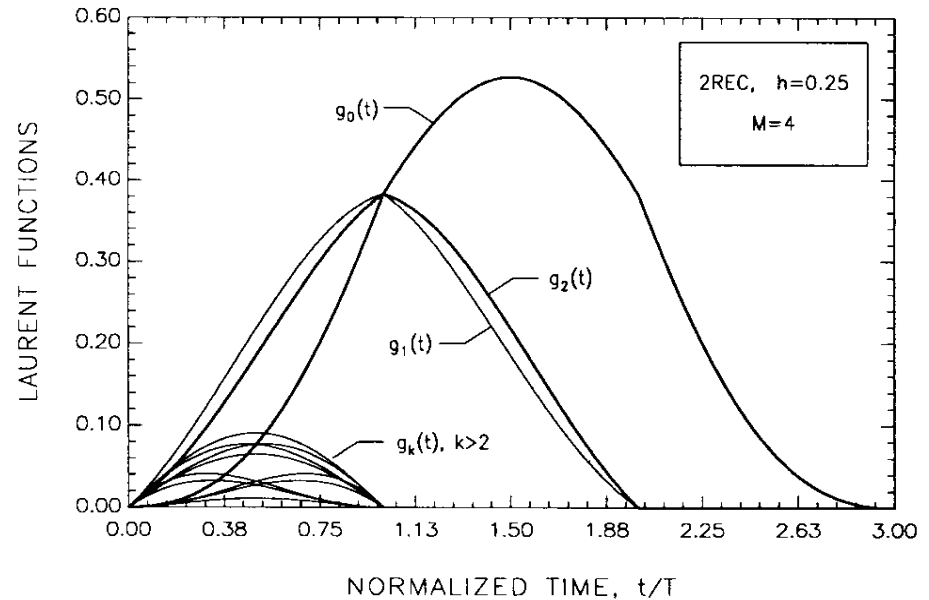
$$\sigma_n = (\dots, \alpha_{n-3}, \alpha_{n-2}, \alpha_{n-1}, \alpha_n) \leftrightarrow \sigma_n = (\underbrace{\phi_{n-L}, \alpha_{n-L+1}, \dots, \alpha_{n-1}, \alpha_n}_{pM^{L-1} \text{ states}})$$



Pulse Amplitude Modulation (PAM) based CPM model

- M-ary Single-h

$$s(t; \alpha) = \sqrt{\frac{E_s}{T_s}} \sum_{k=0}^{N-1} \sum_i b_{k,i} g_k(t - iT_s)$$



- PAM complexity reduction principle

Number of PAM Components $N = 2^{P(L-1)} (M - 1)$ and $P = \log_2 M$

$$s(t; \alpha) = \sqrt{\frac{E_s}{T_s}} \sum_i e^{j\phi_{i-L}} \sum_{k=0}^{N-1} b_k(c_i) g_k(t - iT_s) \quad \kappa \subseteq \{0, 1, \dots, N-1\}$$

- Subset the largest amplitude pulses to reduce the number of matched filters (MF)
- Reduce number of trellis states in the detector

PAM based joint timing and phase error detector

- Received signal model in AWGN channel

$$r(t) = e^{j\theta} \sqrt{\frac{E_s}{T_s}} \sum_{k=0}^{N-1} \sum_i b_{k,i} g_k(t - \tau - iT_s) + w(t)$$

- Coherent detection

- Symbol detection using the Viterbi algorithm (VA)
- Decision-directed timing recovery
- Decision-directed phase recovery

- Noncoherent detection

- Symbol detection using the Viterbi algorithm
- Decision-directed timing recovery without explicit phase information

Note:

- Timing and phase recovery uses decisions from the receiver.
- Symbol detection and signal recovery are based on maximum likelihood principle.

PAM based joint timing and phase error detector

- Metric increment in VA for sequence detection

$$\sum_{i=0}^{L_0-1} \operatorname{Re}\{y_i(\tilde{c}_i, \tilde{\phi}_{i-L}, \tau)e^{-j\theta}\} = 0 \quad 0 \leq t \leq L_0 T_s$$

- PAM-based TED is given by $\dot{y}_i(c_i, \phi_{i-L}, \tilde{\tau})e^{-j\theta} = \sum_{k \in k_{TED}} b_{k,i}^* \dot{x}_{k,i}(\tilde{\tau})$

where the TED increment $\sum_{i=0}^{L_0-1} \operatorname{Re}\{\dot{y}_i(c_i, \phi_{i-L}, \tilde{\tau})e^{-j\theta}\} = 0$

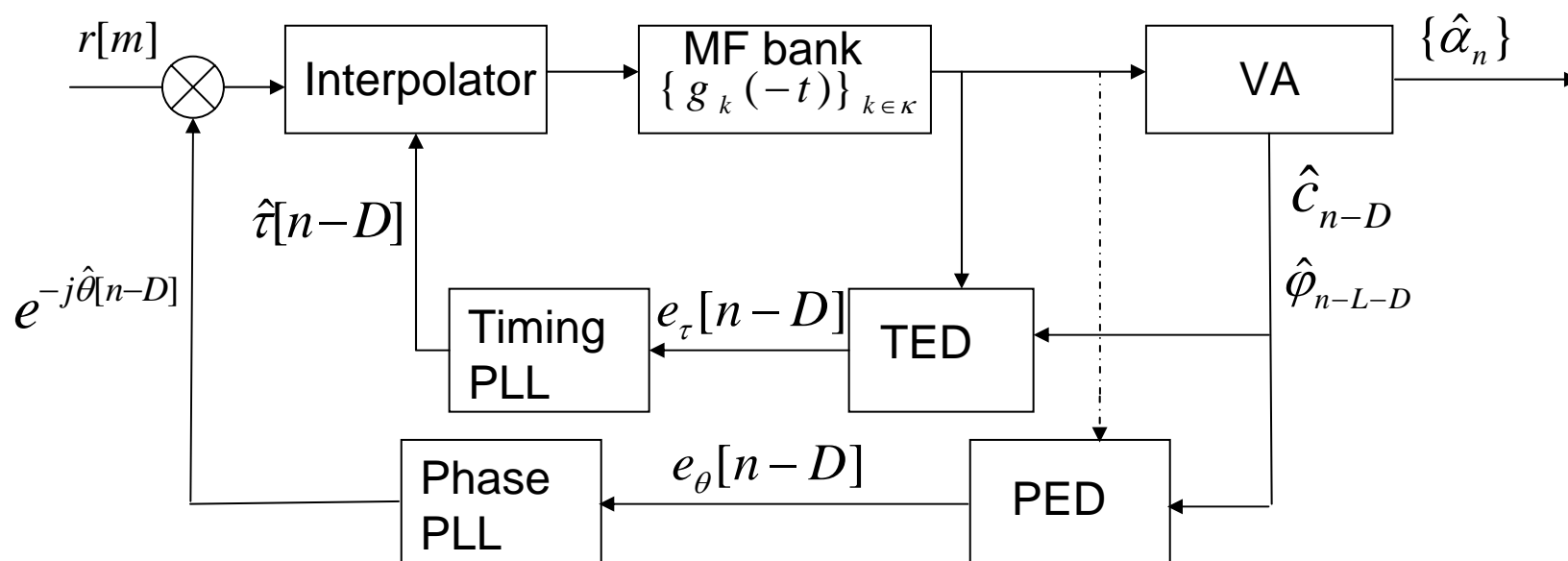
- PAM-based PED is given by $z_i(c_i, \phi_{i-L}, \tau)e^{-j\tilde{\theta}} = \sum_{k \in k_{PED}} b_{k,i}^* x_{k,i}(\tau)$

where the PED increment $\sum_{i=0}^{L_0-1} \operatorname{Im}\{z_i(c_i, \phi_{i-L}, \tau)e^{-j\tilde{\theta}}\} = 0$

MF bank filter output $x_{k,i}(\tau) \cong \int_{\tau+iT_s}^{\tau+(i+D_k)T_s} r(t)e^{-j\theta} g_k(t - \tau - iT_s) dt$

and $1 \leq D_k \leq L+1$

Error detector implementation



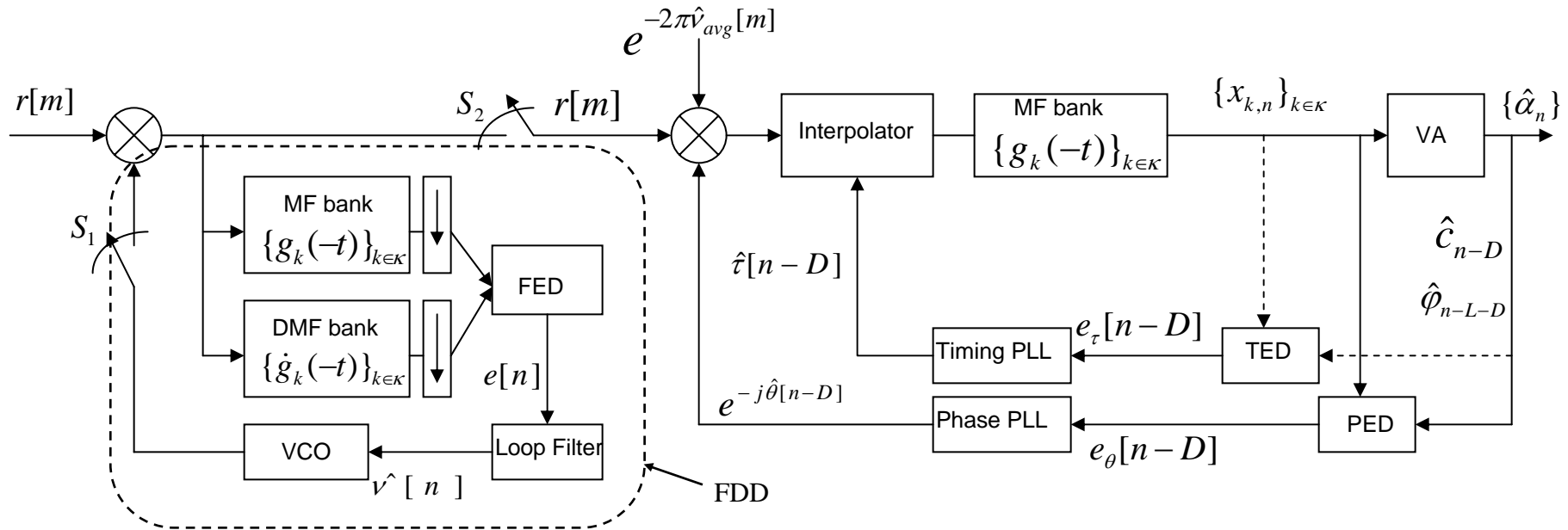
Error signal from the TED $e_{\tau}[n-D] = \text{Re} \left\{ \dot{y}_{n-D}(\hat{c}_{n-D}, \hat{\phi}_{n-L-D}, \hat{\tau}[n-D]) e^{-j\hat{\theta}[n-D]} \right\}$

Error signal from the PED $e_{\theta}[n-D] = \text{Im} \left\{ z_{n-D}(\hat{c}_{n-D}, \hat{\phi}_{n-L-D}, \hat{\tau}[n-D]) e^{-j\hat{\theta}[n-D]} \right\}$

Note:

- Matched filters estimate data symbols through VA implementation.
 - Derivative matched filters generate TED Error hence timing estimate.
- A discrete-time differentiator approximates the derivative.

Effect of large frequency offsets on TED and PED



- Frequency offset on the order of the symbol rate $1/T_s$
 - A non-data-aided (NDA) frequency recovery is done before attempting symbol sequence, timing and phase recovery. A Frequency Difference Detector (FDD) is employed for this purpose.
 - Timing recovery without the explicit recovery of phase (noncoherent) is more suitable as phase recovery is still difficult due to the average residual frequency jitter \hat{v}_{avg} .

Performance analysis metrics and bounds

- We use modified Cramer-Rao bound (MCRB) to establish a lower bound on the degree of accuracy to which τ , θ and ν can be estimated.

- Normalized MCRB - timing $\frac{1}{T_s^2} \times MCRB(\tau) = \frac{1}{8\pi^2 h^2 C_\alpha C_f L_0} \times \frac{1}{E_s / N_0}$
 where $C_\alpha \cong E\{\alpha_n^2\} = (M^2 - 1)/3$ for uncorrelated data symbols
 special cases : 1) LREC: $C_f = C_{LREC} \cong 1/(4L)$

2) LRC: $C_f = C_{LRC} \cong 3/(8L)$

- Normalized timing error variance $\frac{1}{T_s^2} \times \sigma_\tau^2 \cong \frac{1}{T_s^2} \times Var\{\hat{\tau}[n] - \tau\}$

- MCRB – phase $MCRB(\theta) = \frac{1}{2L_0} \times \frac{1}{E_s / N_0}$

- Phase error variance $\sigma_\theta^2 \cong Var\{\hat{\theta}[n] - \theta\}$

- MCRB – frequency $T_s^2 \times MCRB(\nu) = \frac{3}{2\pi^2 L_0^3} \times \frac{1}{E_s / N_0}$

- Normalized frequency error variance $T_s^2 \times \sigma_\nu^2 \cong T_s^2 \times Var\{\hat{\nu}[n] - \nu\}$

Performance analysis metrics and bounds...contd.

- Phase Locked Loop (PLL) Considerations
 - Error detector outputs are refined into suitable offset estimates
 - The loop bandwidth BT_s is an important parameter determining the performance of the synchronizers.
- Timing PLL
 - First order timing PLL implementation refines the TED output $e_\tau[n]$ after every T_s , $\hat{\tau}[n] \cong \hat{\tau}[n-1] + \gamma_\tau e_\tau[n]$, PLL step size is $\gamma_\tau \cong \frac{4B_\tau T_s}{k_{p\tau}}$
- Phase PLL
 - The new phase estimate from the PLL is obtained as $\hat{\theta}[n] \cong \hat{\theta}[n-1] + \gamma_\theta \xi[n]$
 - First order PLL with no carrier frequency offset and $\xi[n] = e_\theta[n]$
 - Second order PLL with residual carrier frequency offset
$$\xi[n] = \xi[n-1] + (K1 + K2)\kappa_{p\theta} e_\theta[n] - K2\kappa_{p\theta} e_\theta[n-1]$$
K1 and K2 are proportional and integration constants respectively
- Frequency PLL
 - First order frequency PLL refines FDD output after every T_s as
$$\hat{\nu}[n] \cong \hat{\nu}[n-1] + \gamma_\nu e_\nu[n].$$
 PLL step size is $\gamma_\nu \cong \frac{4B_\nu T_s}{k_{p\nu}}$

Performance analysis metrics and bounds...contd.

- S-Curve identifies the stable lock points
 - These are the zero-crossing positive slope points on the curve.
 - We want the such a point at zero error, otherwise it is a false lock point
 - Decision directed M-ary TED and PED have false lock points
 - FDD is NDA, therefore, free of false lock points.

- S-curve for TED

$$- S(\delta_\tau) \cong \sqrt{E_s / T_s} \cdot E\{e_\tau[n] | \delta_\tau\}$$

where $\delta_\tau \cong \tau - \hat{\tau}$ is timing offset

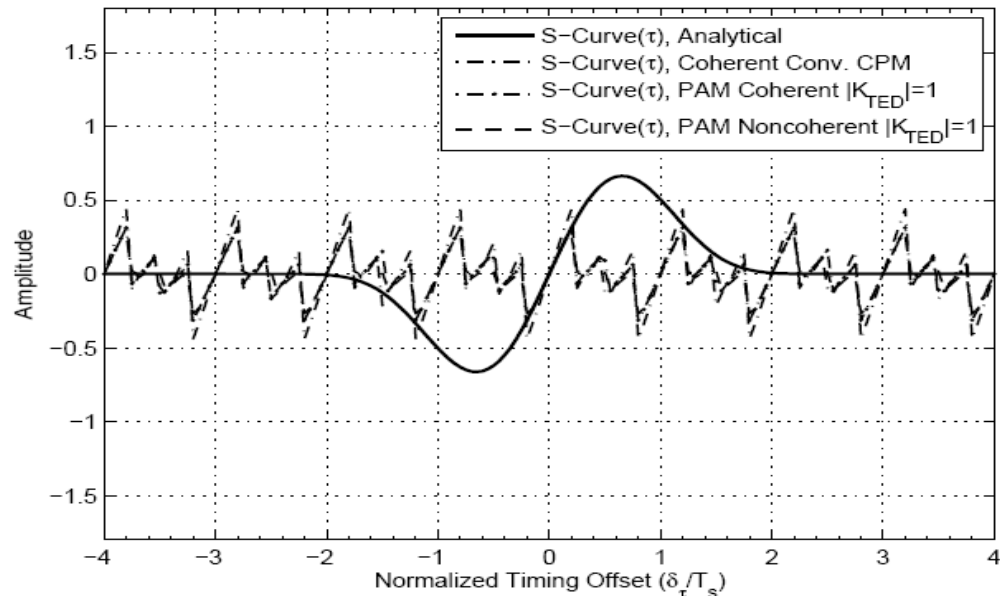


Figure 6.6. S-Curves for the TED. The modulation scheme is Quaternary CPM ($M = 4, L = 2, h = 1/4$).

Performance analysis metrics and bounds...contd.

S-curve for PED

$$- S(\delta_\theta) \cong \sqrt{E_s/T_s} \cdot E\{e_\theta[n] | \delta_\theta\}$$

where $\delta_\theta \cong \theta - \hat{\theta}$ is the phase offset

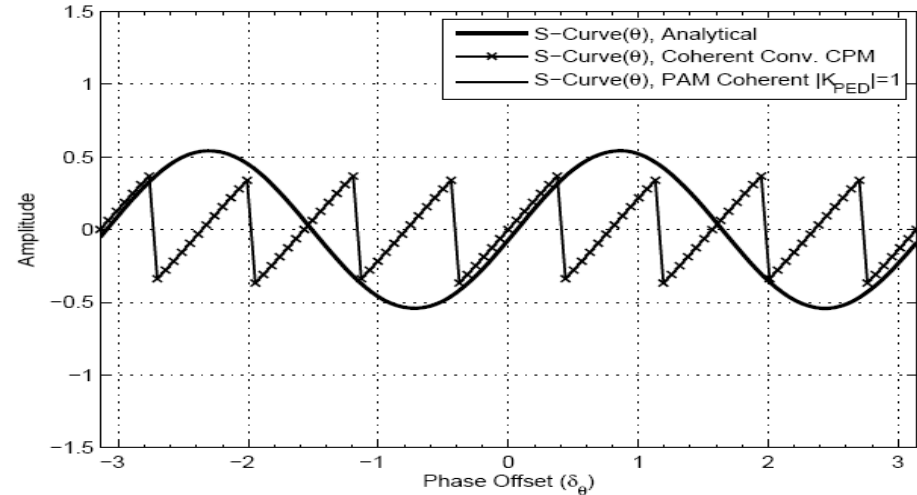


Figure 6.7. S-Curves for the PED. The modulation scheme is Quaternary CPM ($M = 4, L = 2, h = 1/4$).

•S-curve for FDD

$$- S(\delta_\nu) \cong \sqrt{E_s/T_s} \cdot E\{e_\nu[n] | \delta_\nu\}$$

where $\delta_\nu \cong \nu - \hat{\nu}$ is the frequency offset

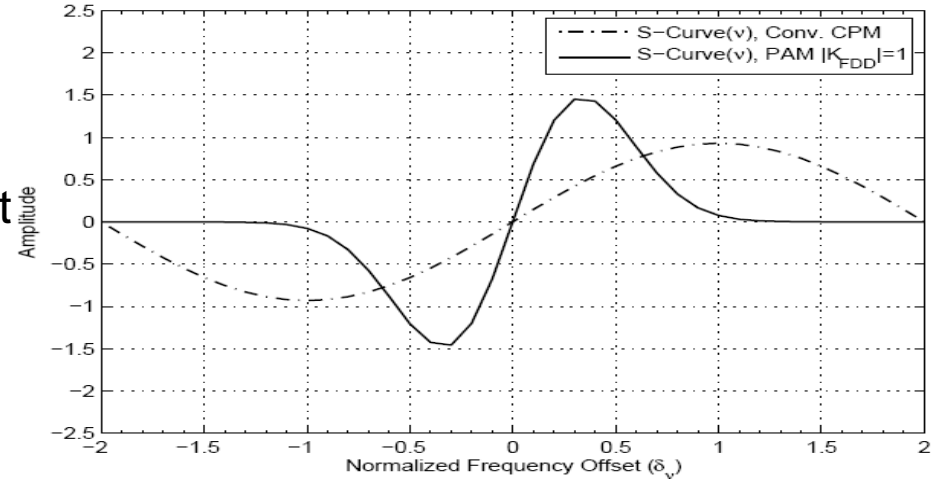


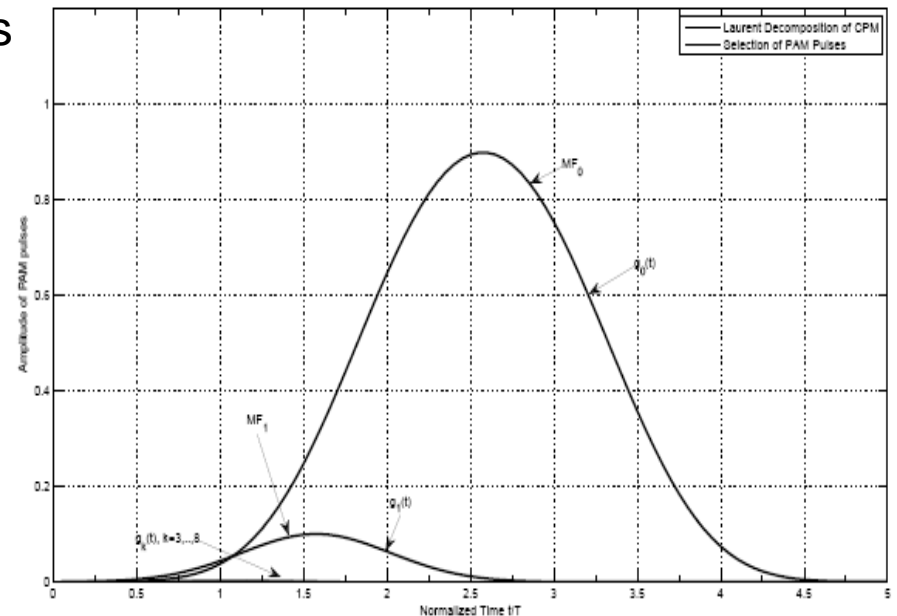
Figure 6.15. S-Curves for the FDD. The modulation scheme is M -ary CPM ($M = 4, 2RC, h = 1/4$).

Simulation results

- Binary GMSK system with Gaussian pulses
(Gaussian Minimum Shift Keying)

M=2, 4G, h=1/2

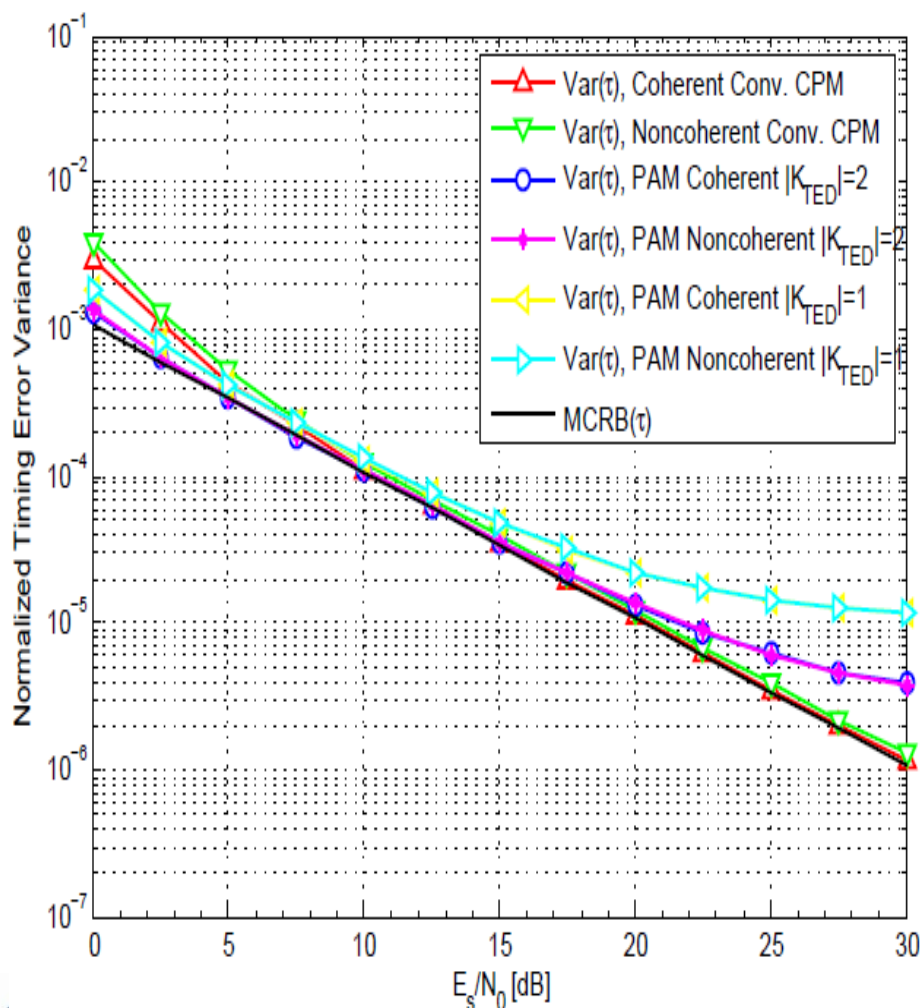
- Optimal PAM based detector
 - Trellis state = 16
 - 8 single-h MFs/Pulses



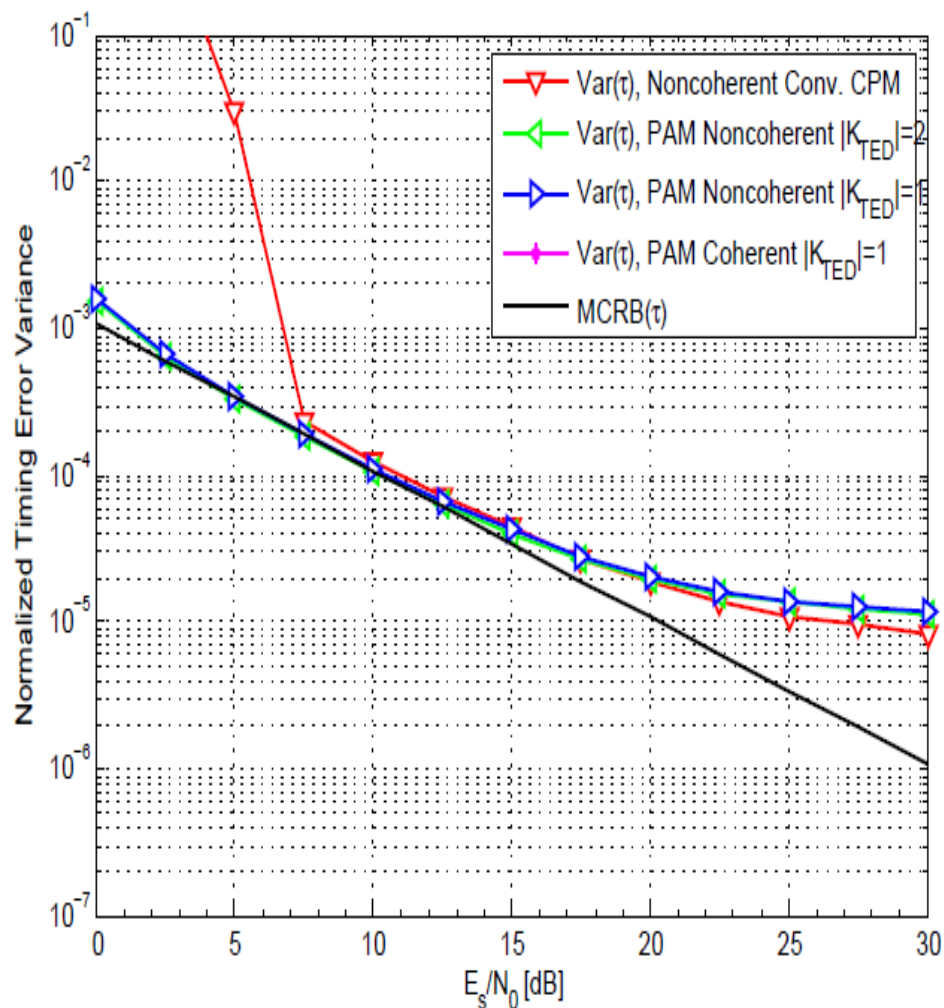
- Reduced complexity detectors chosen for this example
 - 4 state detector with $L' = 2$
 - $|\mathcal{K}| = |\mathcal{K}_{TED}| = |\mathcal{K}_{PED}| = 2$ MFs/pulses.
 - $|\mathcal{K}| = 2$ MFs and $|\mathcal{K}_{TED}| = |\mathcal{K}_{PED}| = 1$ pulse.

Simulation results (Binary GMSK...)

• Timing error variance with no carrier frequency offset

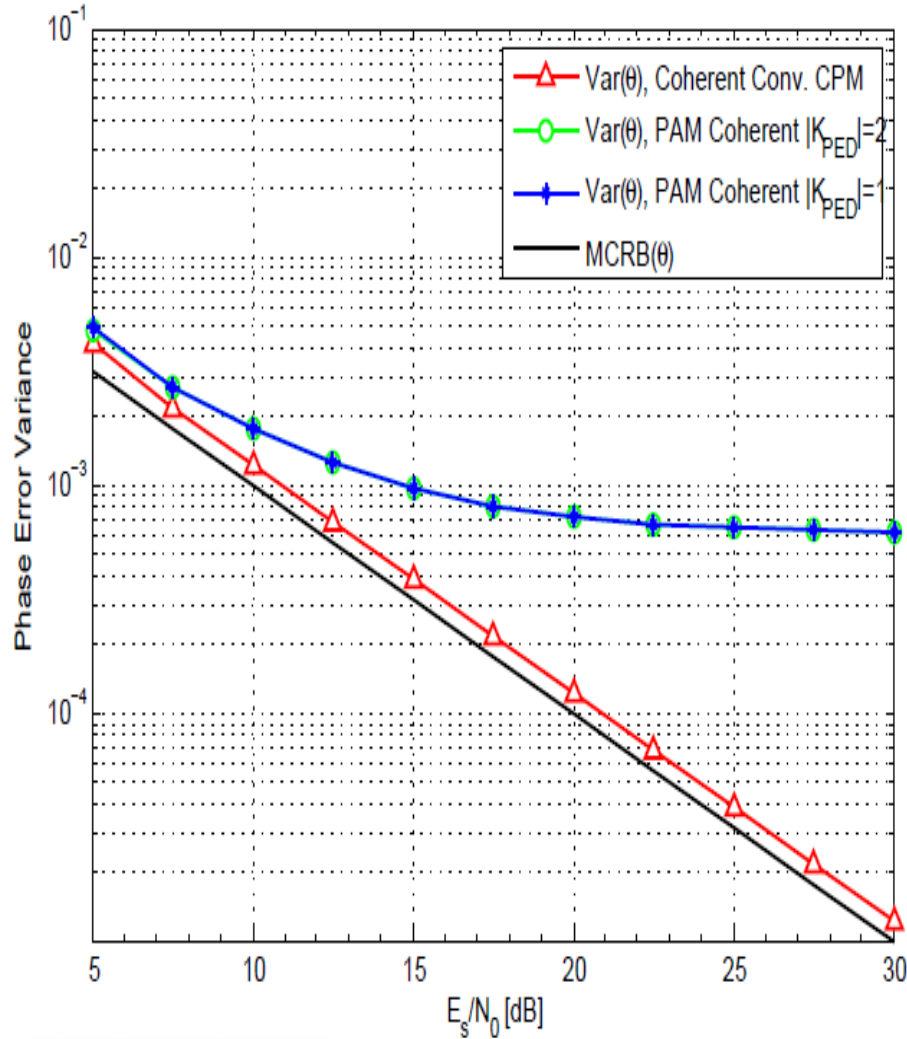


• Timing error variance with a large carrier frequency offset

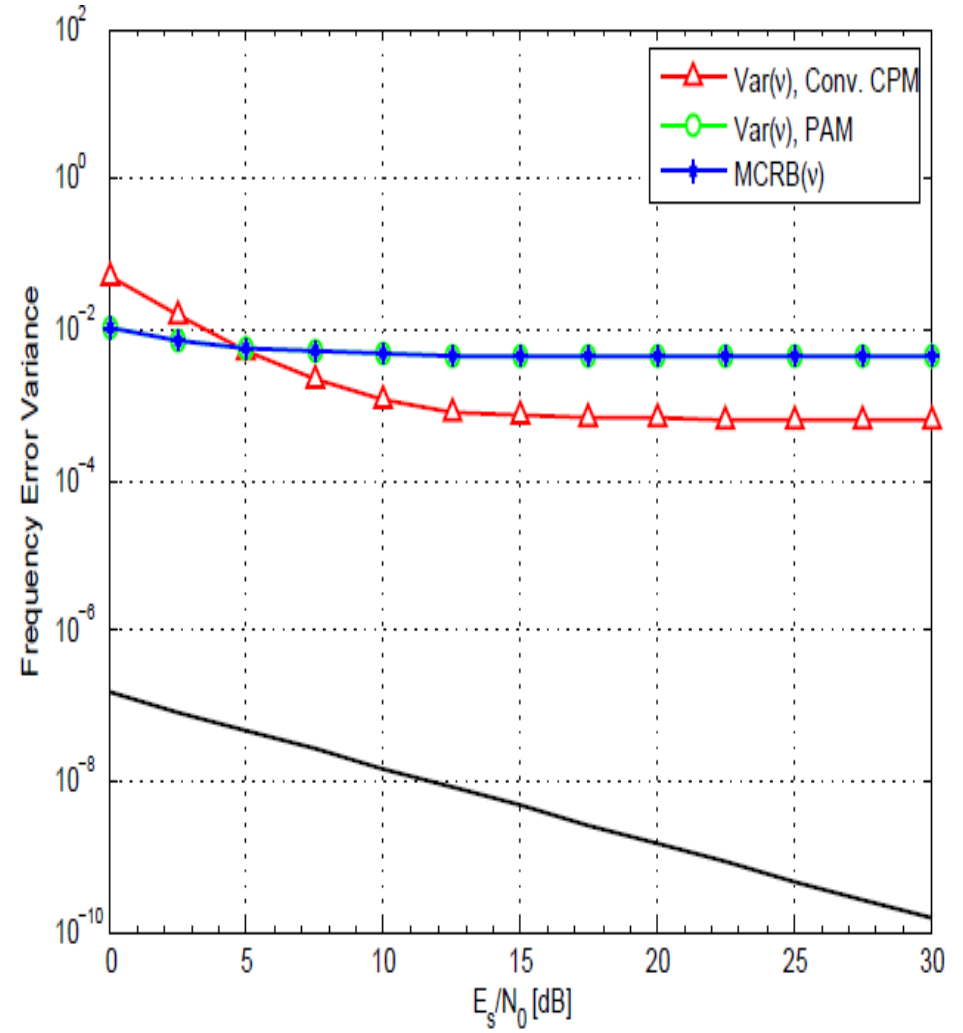


Simulation results (Binary GMSK)

•Phase error variance with no carrier frequency offset

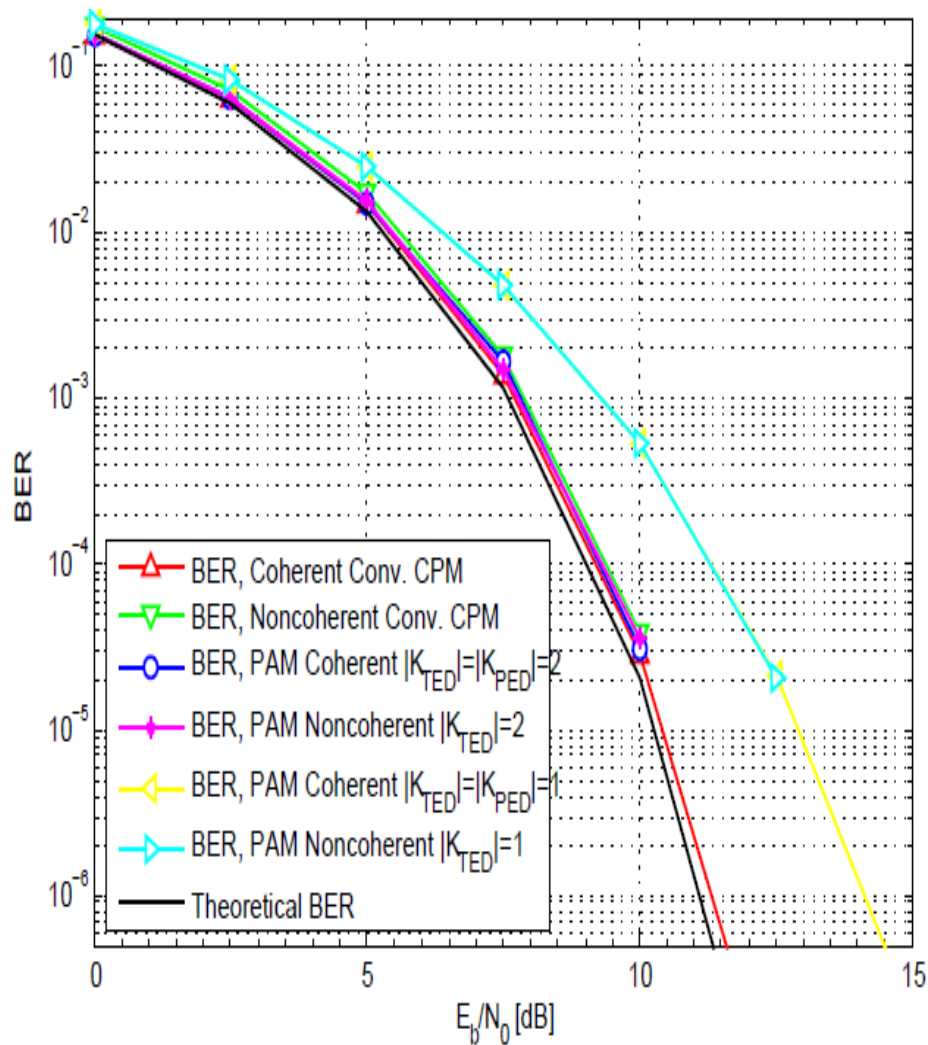


•Frequency error variance with a large carrier frequency offset

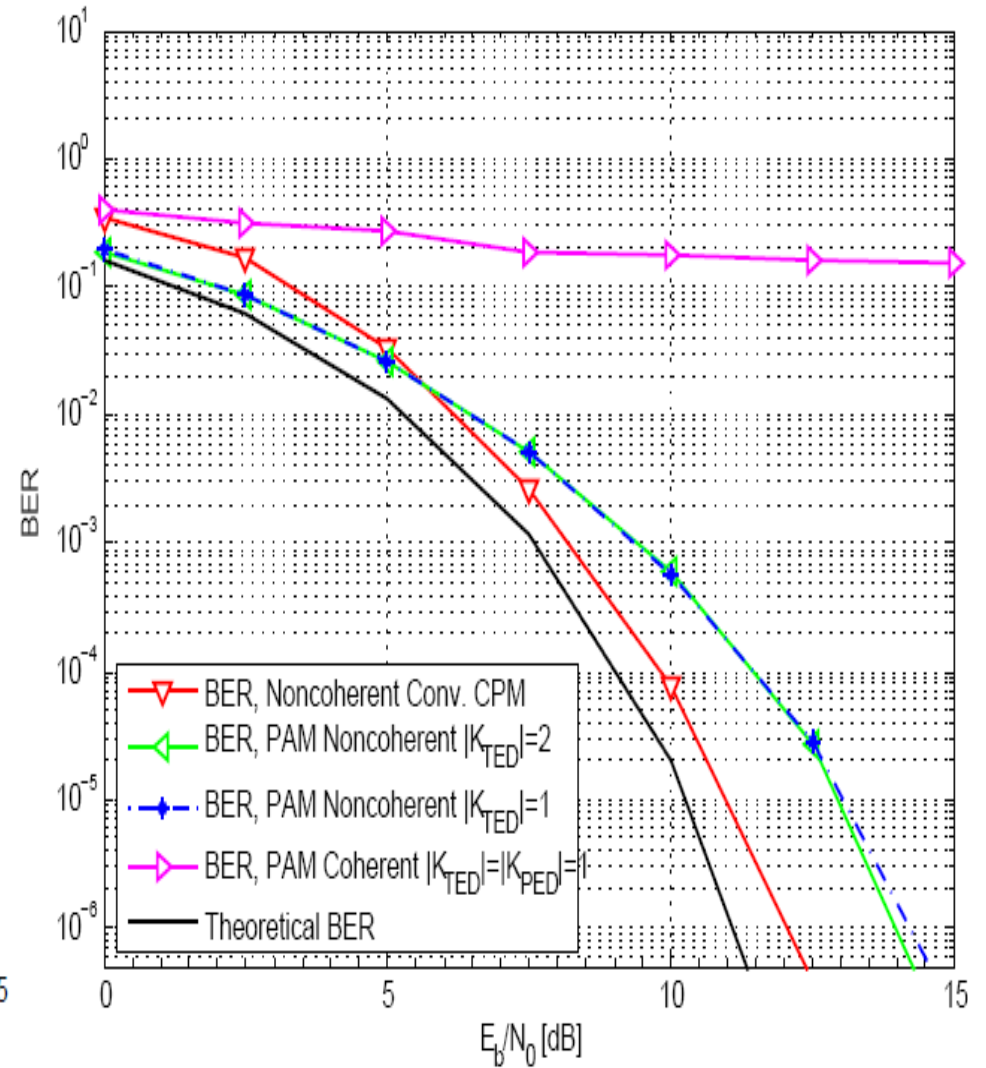


Simulation results (Binary GMSK)

• BER with no carrier frequency offset



• BER with a large carrier frequency offset

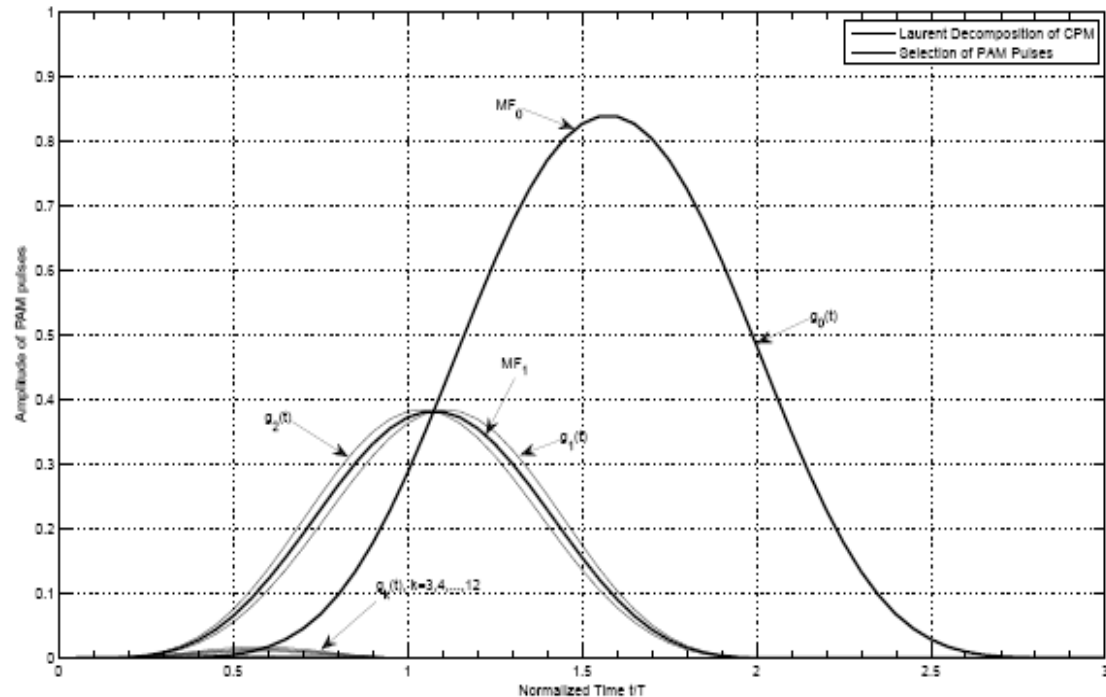


Simulation results

- M-ary CPM system with partial response

M=4, 2RC, h=1/4

- Optimal PAM based detector
- Trellis state = 16
- 12 single-h MFs/Pulses

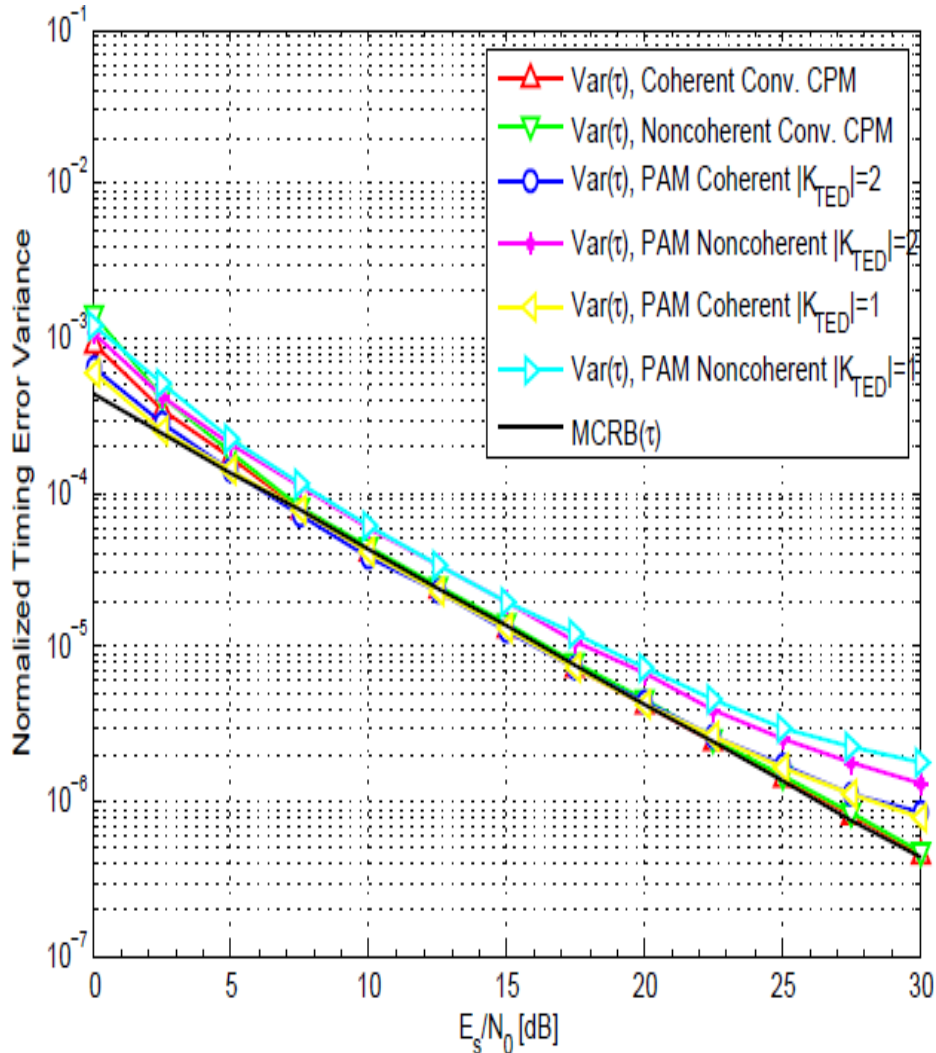


Reduced complexity detectors chosen for this example

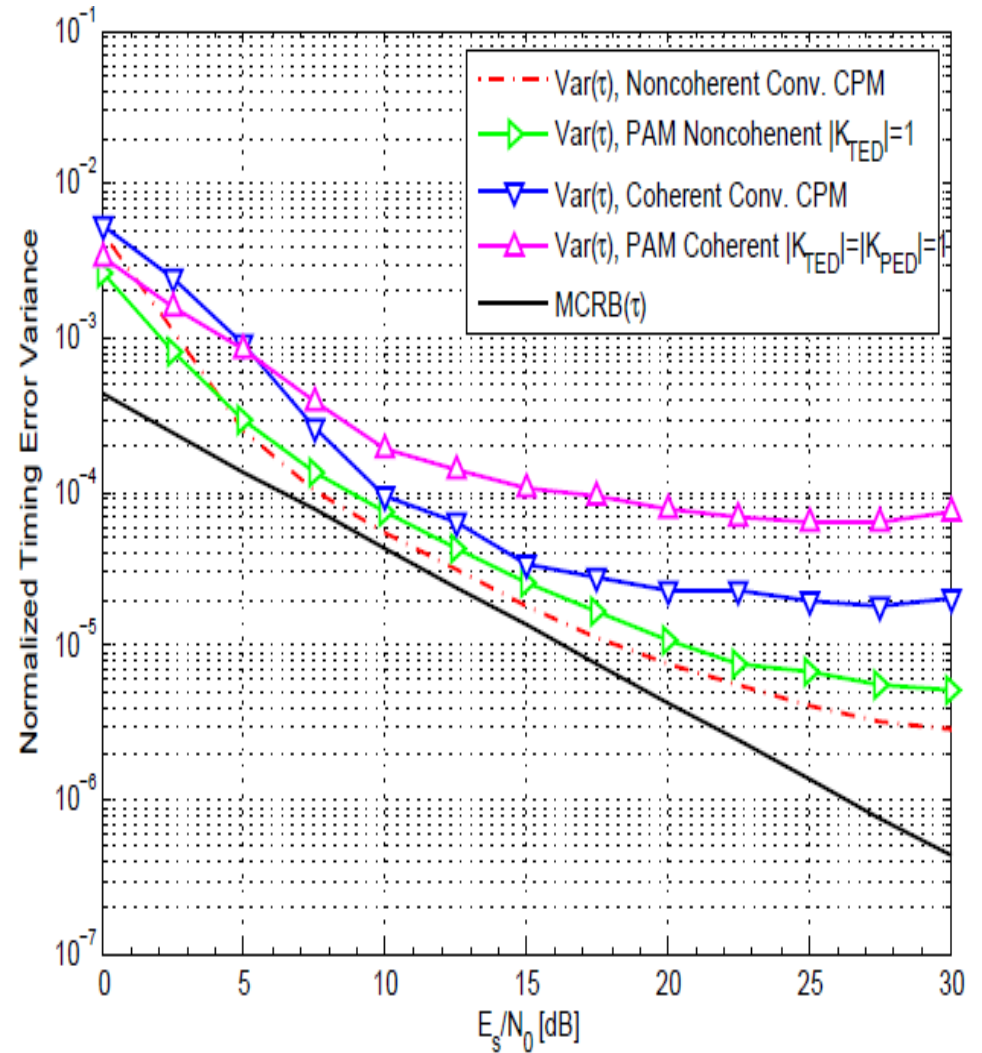
- 4 state detector with $L' = 1$
- $|\mathcal{K}| = |\mathcal{K}_{TED}| = |\mathcal{K}_{PED}| = 2$ MFs/pulses.
- $|\mathcal{K}| = 2$ MFs and $|\mathcal{K}_{TED}| = |\mathcal{K}_{PED}| = 1$ pulse.

Simulation results (M-ary CPM...)

• Timing error variance with no carrier frequency offset

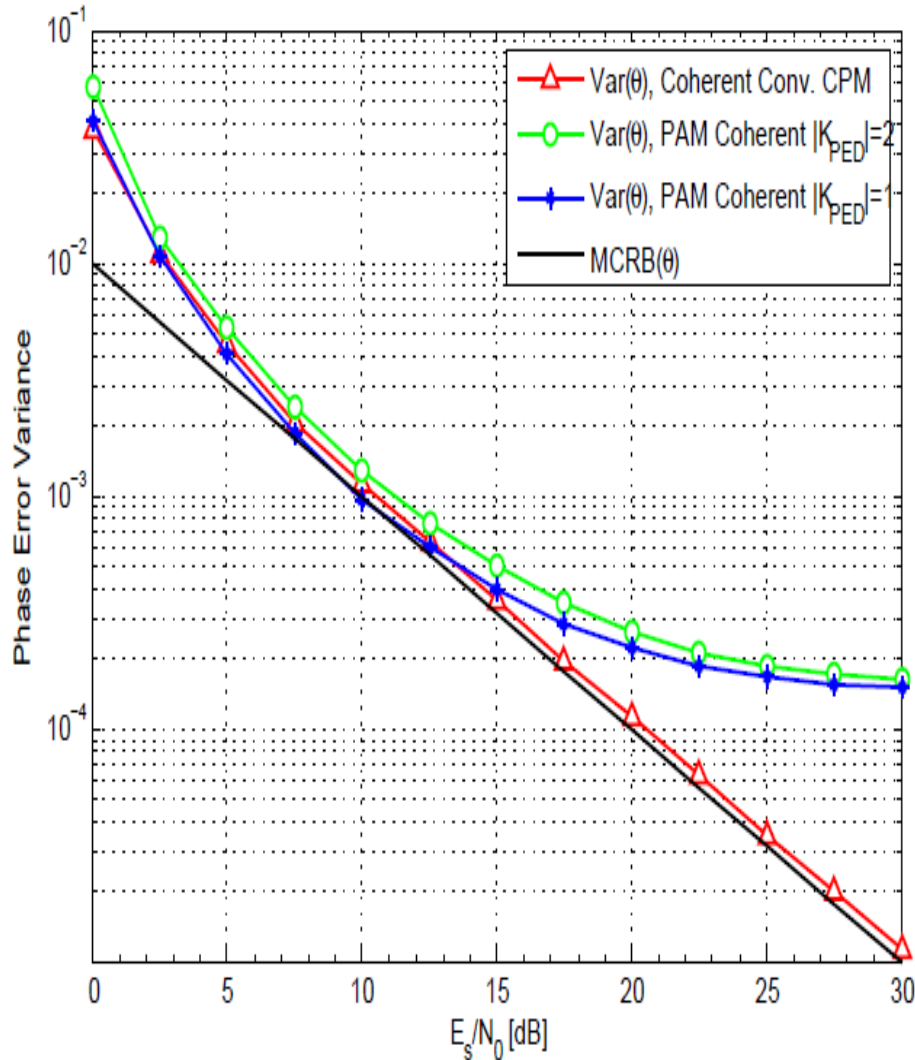


• Timing error variance with a large carrier frequency offset

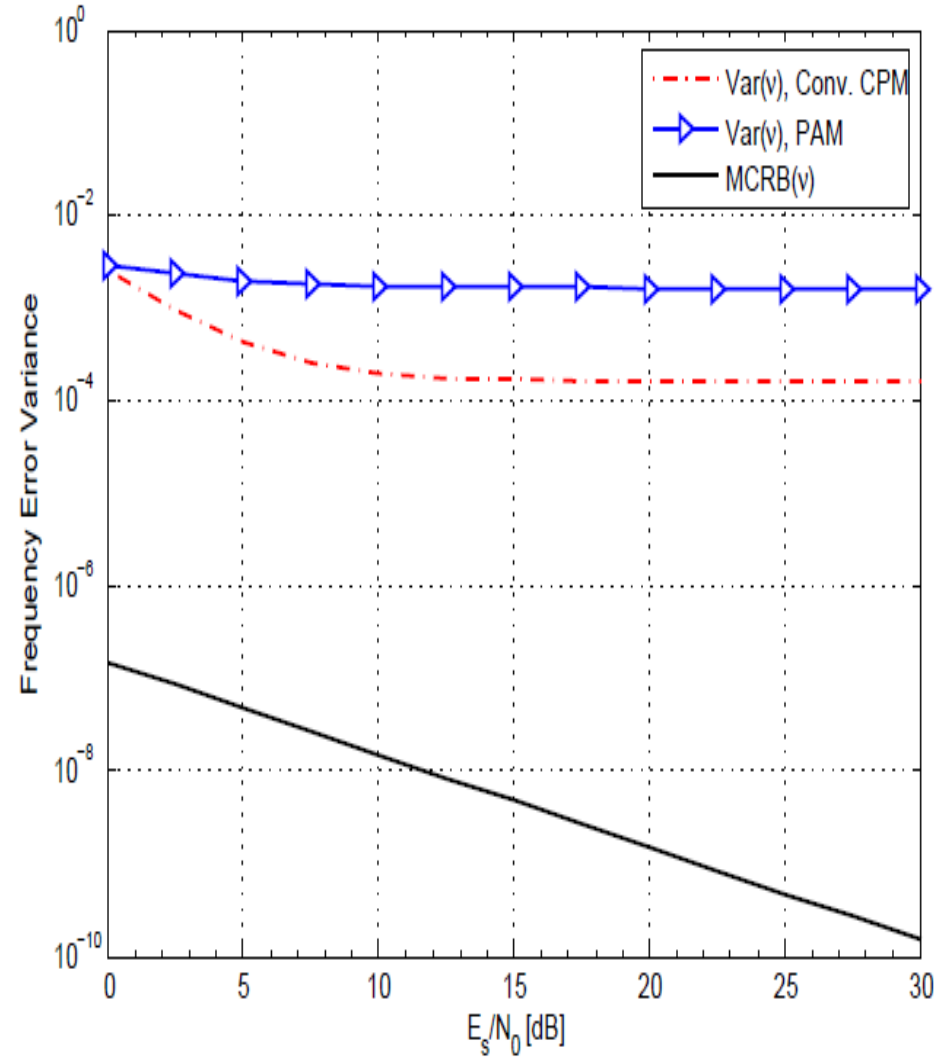


Simulation results (M-ary CPM...)

• Phase error variance with no carrier frequency offset

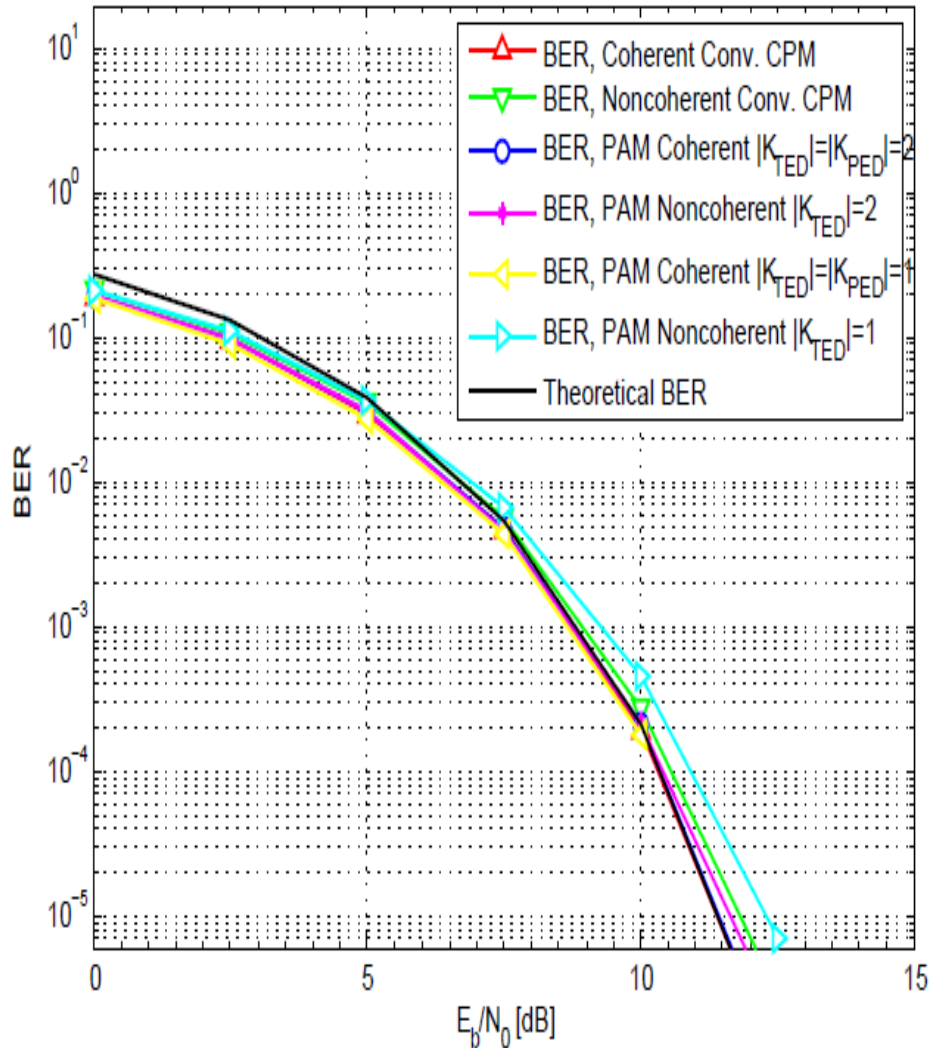


• Frequency error variance with a large carrier frequency offset

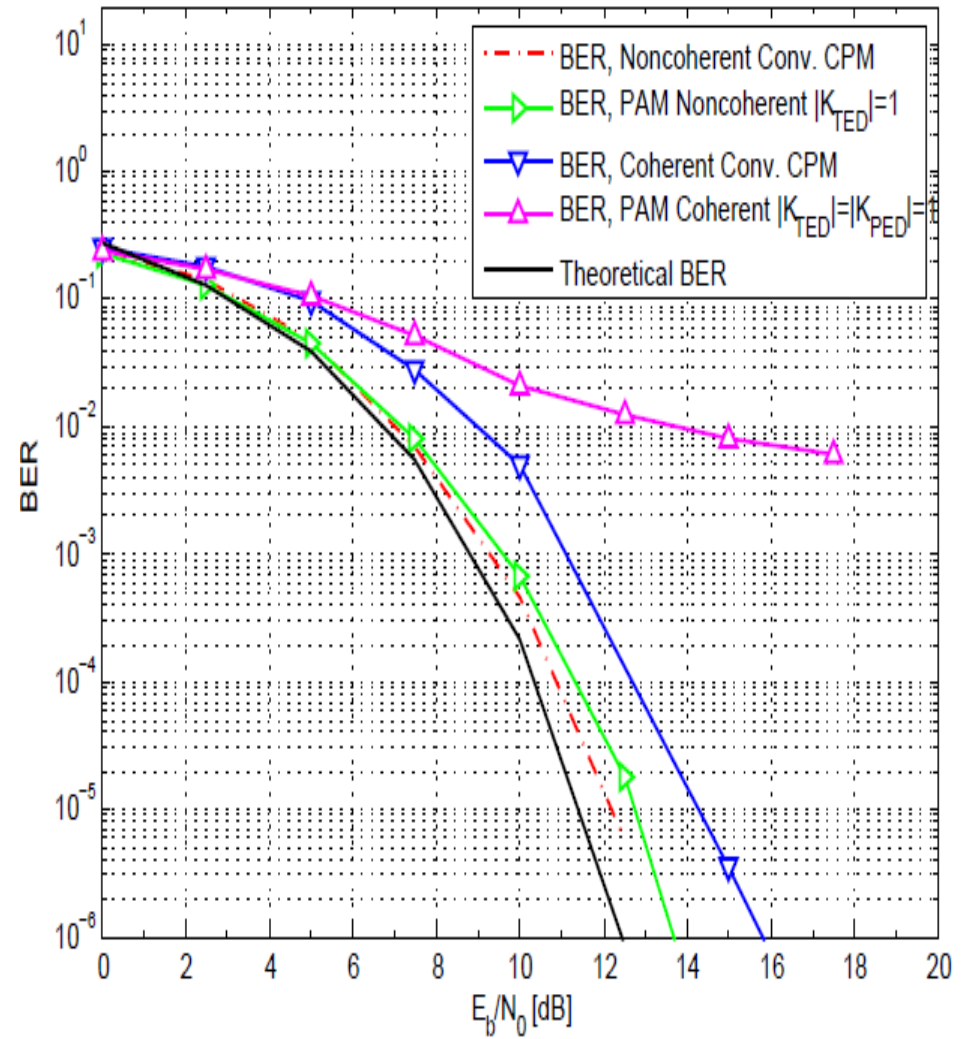


Simulation results (M-ary CPM...)

•BER with no carrier frequency offset



•BER with a large carrier frequency offset



Summary of simulation results

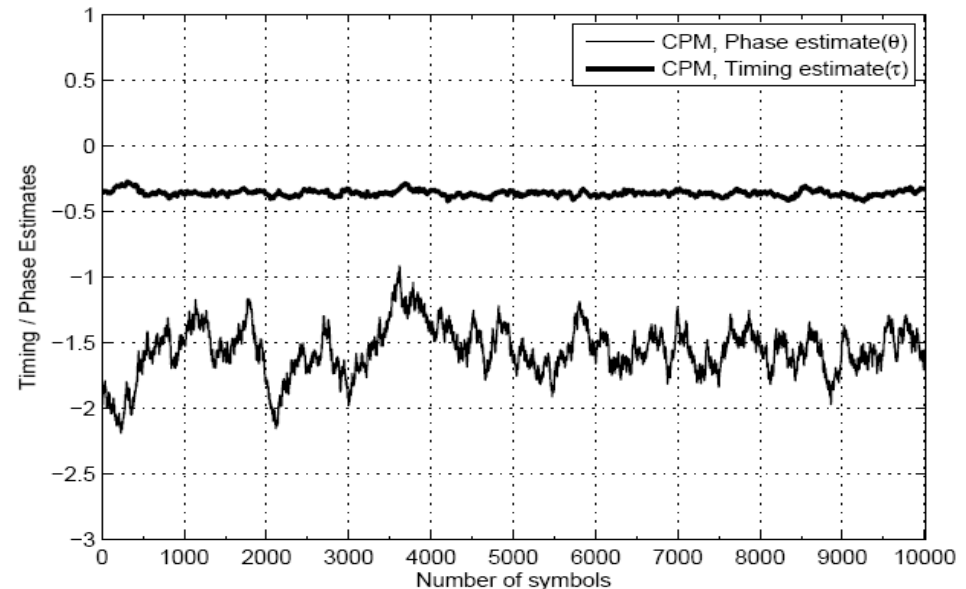
- PAM based reduced-complexity CPM detectors provide very good tracking characteristics under no carrier frequency offset.
- Coherent and noncoherent detection can be done based on PAM based detectors. The noncoherent detectors are worse by about 2-3 dB in BER under all practical requirements and under no frequency offset condition.
- With a frequency offsets on the order of 10^{-4} of the symbol rate, the performance of PAM based detectors does not suffer deterioration in terms of tracking accuracy and BER.
- With the carrier frequency offset on the order of the symbol rate, noncoherent detection outperforms coherent detection in terms of tracking accuracy and BER.
- Noncoherent detection allows further simplification of the receiver structure by alleviating the need for a second stage of frequency recovery.

False lock recovery using reduced complexity detector configurations

- M-ary partial response CPM systems suffer from false lock problems during signal acquisition.
- Under false lock, the synchronizers settle at incorrect timing and phasing instants rendering poor BER, timing and phase error variance.
- NDA auxiliary lock detectors remove false locks but has a longer acquisition time.

CPM (M=4, 3RC, h=1/2)

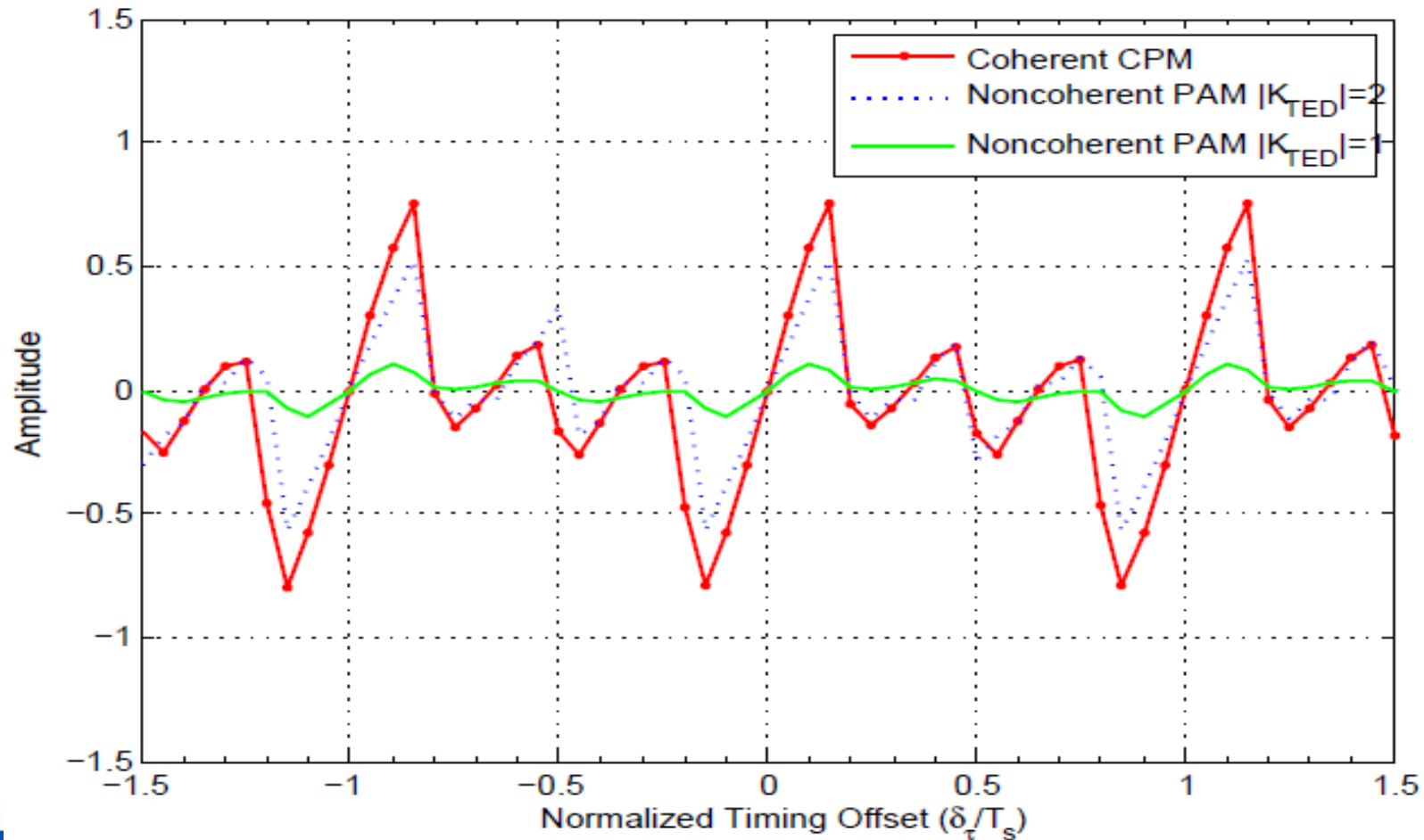
Metric	Value by Simulation	Theoretical
BER	0.2808	0
Timing Variance	0.5007×10^{-3}	0.0511×10^{-3}
Phase Variance	0.0397	0.0006



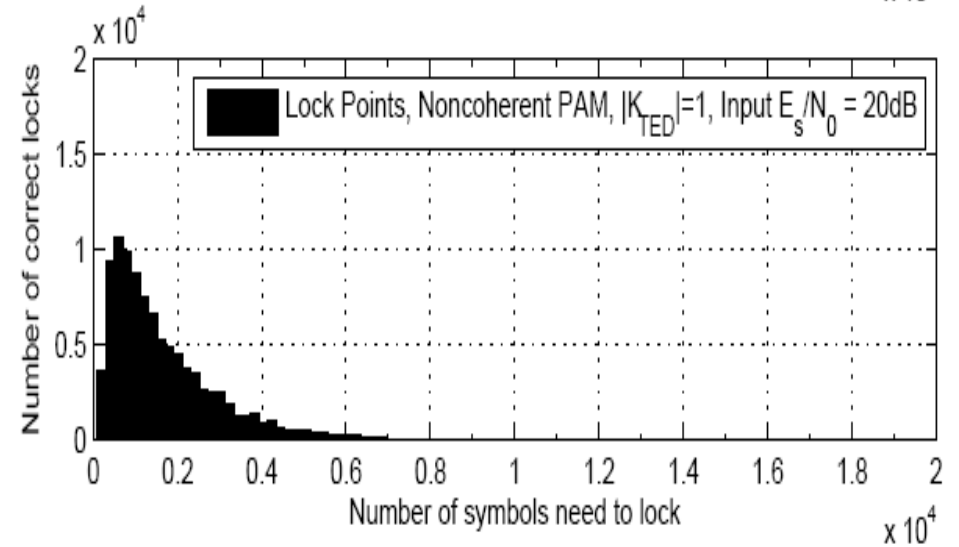
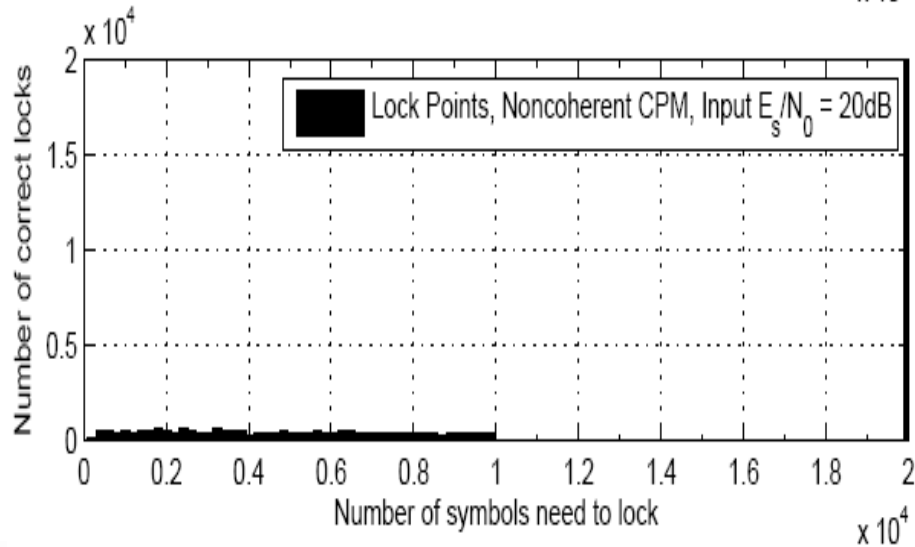
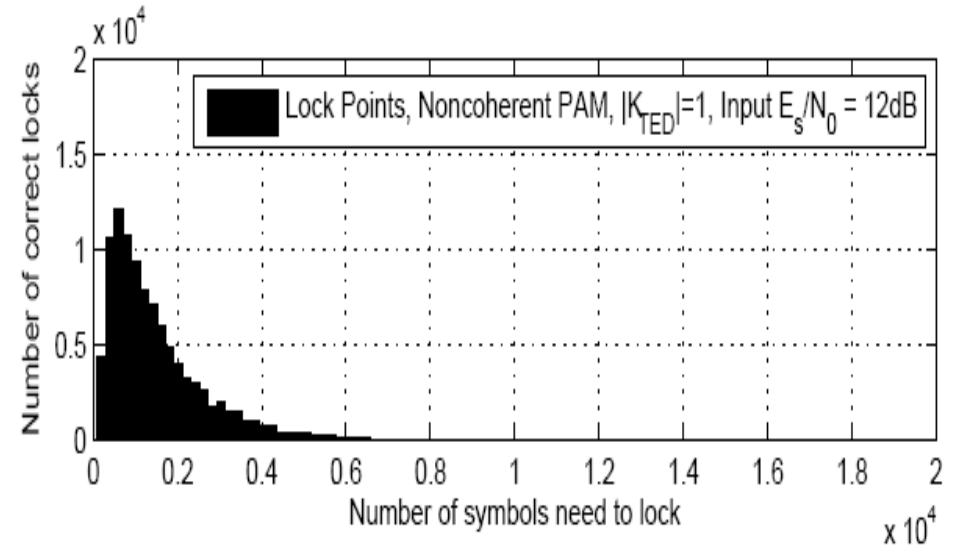
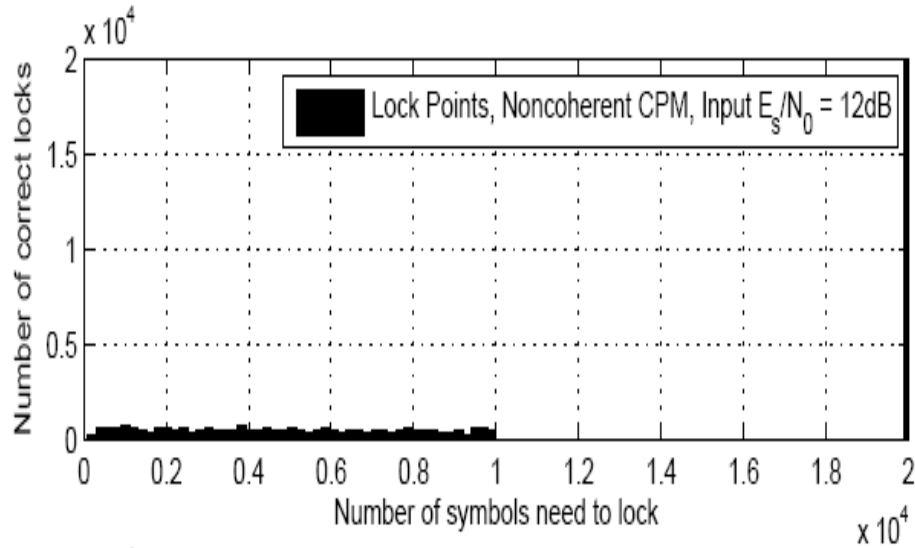
Due to the variable lengths of the PAM filter components, PAM based configurations can deal with this problem more effectively than its conventional CPM counterpart.

False lock recovery ... contd.

- S-curves for M-ary CPM (M=4, 3RC, h=1/2)



False lock recovery ... contd.



False lock recovery ... contd.

- Observations

- CPM (M=4, 3RC, h=1/2), conventional and PAM based with 1 pulse noncoherent TED with $B_{\tau}T_s = 5 \times 10^{-3}$ during initial acquisitions.

No Frequency Offset	Noncoherent conventional	Noncoherent PAM $ \mathcal{K}_{\text{TED}} = 1$
No. of Simulations	10^5	10^5
No. of False locks	10^5	30
False lock probability	1	0.0003
Lock state	No lock	Consistent over no. of symbols

Conclusions and future work

•Conclusion

- Synchronizers provide a comparable performance against conventional CPM receivers.
- Under a large carrier frequency offset, a PAM based receiver in noncoherent mode offer similar performance as its CPM counterpart
- A novel method of decision-directed false lock recovery for PAM based CPM receivers.

• Future work

- Joint phase and timing recovery in wireless fading channels.
- Possibility of different PAM based error detector configurations for acquisition and tracking stages.

Acknowledgements

I would like to thank

- My Advisor, **Dr. Erik Perrins**
- Committee members **Dr. Sam Shanmugan** and **Dr. Shannon Blunt**
- **Nokia-Siemens Networks** and **The University of Kansas General Research Funds** for their support throughout this research
- Communication theory and systems research group at KU
- Family and friends

Thank you!

Questions??